Paper No.
MCI31

Metal-Microbe Synergy Mechanisms in Localized Corrosion of Stainless Steels

R. P. George

Corrosion Science & Technology Division
Indira Gandhi Centre for Atomic Research
Kalpakkam 603102
INDIA

U. Kamachi Mudali

Materials Chemistry and
Metal Fuel Cycle Group
Indira Gandhi Centre for Atomic Research
Kalpakkam 603102
INDIA

B. Anandkumar

Corrosion Science & Technology Division
Indira Gandhi Centre for Atomic Research
Kalpakkam 603102
INDIA

ABSTRACT

Stainless steels (SS) are the favourite materials for industrial application due to its outstanding mechanical properties, weldability and general corrosion resistance. However, corrosion resistance offered by a few nanometer thick chromium oxide passive film is under threat from both the environmental and metallurgical variables. Stainless steels are susceptible to localized corrosion especially under the influence of chlorides and bioflms. Researchers worldwide have attempted to understand the critical factors involved in localized corrosion of SS. Earlier it was assumed that the quality of the passive film is the critical factor and the quality of the passive film depends on the metallurgical factors. However studies also showed that integrity of passive film is crucial only for pit initiations. The environmental factors play a major role in maintaining pit propagation especially chlorides and microbes. In many aqueous environments major localized corrosion damage were reported under biofilms formed by microorganisms. Advanced SS developed with high pitting resistance equivalent number (PREN) for sea water applications have failed due to crevice corrosion under biofilms. Even in fresh water environments where concentration of aggressive chlorides ions are below critical level anion-selective biofilms can cause pit stabilization and propagation. An attempt was made to come up with a metal-microbe synergy mechanism for the localized corrosion of SS by manganese oxidizing bacteria and presented in this paper.

Key words: Stainless Steels, Pitting Corrosion, Biofilms, Manganese Oxidizing bacteria

INTRODUCTION

Due to its outstanding general corrosion resistance, weldability, mechanical properties and fabrication costs, stainless steels (SS) are the favorite material for industrial applications. However their susceptibility to localized corrosion and failures due to through wall pitting even in low chloride environment is a serious concern which needs international attention. The corrosion resistance of stainless steels depends upon a thin passive film of a few nanometer thick chromium oxide (Cr_2O_3). Corrosion scientists in early days assumed that quality of the passive film is the critical factor that initiates localized corrosion. However, according to Newman[1], passive film is not all that influences localized corrosion and initiation sites are exclusively at non-metallic inclusions. The steel quality and processing determines the second phases formed either large or small, round or flat, MnS type or other inclusions. Attempts to reduce second phases by sputter deposition and laser surface melting drastically increase pitting resistance of even basic austenitic grades.[2-4] These workers also emphasized that pitting cannot start until an accumulation of a specific local environment occurs resembling a crevice-like cavity and in that sense all pitting is crevice corrosion. Again all crevice or under-deposit corrosion is initiated by pitting. Newman and his group[5] also opined that the effect of different variables on pitting is directly correlating correlated with pit propagation and stability than on pit initiation.
Microbes present in the environment are living agents of corrosion. If the environment supports the metabolic activities of microorganisms and material is susceptible, microbiologically influenced corrosion (MIC) is inevitable. Microbes are small in size, typically in the order of 1-3 碌 m and this small size enables them to access structural flaws and inhomogeneity inhomogeneities on the material surface not apparent at macroscopic level. Microbes tolerate a wide range of pH and oxygen concentrations and can adapt to any aggressive conditions by in vivo genetic engineering. Microbes are implicated In many cases of localized corrosion of stainless steels

Metal-oxidizng and sulfate reducing bacteria have been reported to cause corrosion of stainless steels especially at weld seams in fabricated components.[8] It was assumed that roughness at welds promote microbial attachment. SS with Mo that exhibited good corrosion resistance in seawater also undergoes MIC.[8] According to Walsh and his group, microbes localize and accelerate corrosion in many ways;

they form concentration cells, differential aeration cells, reduce polarization, directly oxidize/reduce metallic atoms/ions, produce corrosive metabolic products like sulphides, promote passive accumulation of anions that will disrupt passive films.[8] In general, the initial attachment of microbes is often random. However further proliferation and biofilm formation is determined by the proximity to metallurgical features that promote the production of high concentration of metabolites.

Localized Corrosion of Stainless Steels

Some major attempts were made by well-known groups to solve the mystery of the localized corrosion process of stainless steel.[9-20] Newman[1] found that the anodic kinetics of the metal in the already developed microenvironment of a pit can account for the effects of a large number of variables in pitting corrosion. The critical pitting potential is associated with the inability of metal to maintain active dissolution as the pit repassivates. Also crevice corrosion is easier than pitting corrosion because the associated diffusion length is longer and required anodic current densities are smaller According to Ryan et al.[9] MnS inclusions play a critical role in pitting and vast majority of pitting events occur at or adjacent to such second phase particles. They used nano-metre scale secondary ion mass spectrometry to demonstrate reduction of Cr-Fe ratio in the steel matrix surrounding MnS particles. It is well known that pitting corrosion of stainless steels at the MnS inclusions can be stimulated by adding chloride ions to the electrolyte.[10] A premature failure of 304 SS pointer rod of a thermostatic mixing valve was attributed to the combined effects of large amounts of MnS inclusions and presence of deformation induced martensite under the influence of chloride environment.[11] However, in all aqueous environments major localized corrosion damages were reported under biofilms formed by microorganisms. Microorganisms on the metal surface creates localized changes at the metal-biofilm interphase with respect to concentration of aggressive anions like oxygen, chlorides, sulfide and pH and accelerate anode formation leading to localized corrosion.[12] It is generally understood that these microorganisms and their metabolic activities severely affect the anodic and cathodic reactions and thus modify the chemistry of any protective layers leading to acceleration of localized corrosion.[6] Suleiman et al.[13] showed that inorganic deposits with anion selective character can stabilize pitting corrosion propagation and decrease corrosion current., Newman[1] explained that biological deposits with anion selective character can also behave in a similar way.

Dickinson et al. **[14]** has proposed that biologically produced MnO_2 augmented with chemical MnO_2 production which can enhance cathodic current and thereby cause ennoblement of SS, this aggravates the concern of E_{corr} exceeding critical pitting potential and enhancing risk of localized corrosion. Many early works have shown that manganese and iron oxides cathodically depolarize SS surfaces and many bacteria like *Leptothrix* sp. can deposit these oxides onto material surfaces by way of biomineralization processes.**[15]** Lewandowski and his group[16] have systematically explored ennoblement of 316L SS by microbially deposited manganese oxides. They have observed an ennoblement of 500 mV increasing the risk of localized corrosion by reaching critical pitting potential. These group of workers advocated ennoblement due to biomineralization by manganese oxidizing bacteria (MOB) as the chief reason leading to localized corrosion of SS. Walsh and group has extensively worked on the relationship between microstructure and microbial interaction.[8] They observed the concentration of biomass at the

fusion boundary and partially melted zone in a low-alloy steel and localized attachment at an autogenous weld in Al2219-T87.They summarized that weld regions are particularly attractive to microbes.

Among the different microorganisms in nature, MOB has great affinity for stainless steels. Dexter et al.[17] reported presence of a group of filamentous manganese oxidizing species of microbes like *Gallionella, Leptothrix, Sphaerotilus, Siderocapsa, Clonothrix,* and *Crenothrix* on SS surfaces. Earlier studies in our laboratory had clearly indicated the favourable adhesion of manganese oxidizing bacteria (MOB) *Leptothrix* sp. and *Bacillus flexus* on 304 SS surfaces and acceleration of pitting.[18,19] The role of MnS inclusions was confirmed by adhesion studies at different applied potentials, surface characterization studies using SEM and EDAX, and immersion pitting studies with ferric chloride solution. Yuan and Pehkonen [20] observed corrosion of SS under the biofilms of manganese oxidizing *Bacillus* sp. Thus the work done by different schools have come up with different mechanisms considering microstructural factors, critical role played by MnS inclusions, biofilms of MOB, and ennoblement due to biomineralization in isolation.

In the present work we have attempted to identify the metal-microbe synergy in localized corrosion of stainless steels using advanced surface characterization and molecular biology tools. The metal-microbe synergy parameters evaluated are favourable adhesion by metal-oxidizing microbes especially Manganese oxidizers, location of adhesion closer to microstructural features, correlation with chemistry of surfaces, aggregation and biofilm formation; growth parameters; microbial diversity in natural biofilms; electrochemical corrosion parameters, locations of pit initiation and pit morphology. Two stainless steels with widely varying Mn alloying content (AISI 202 and AISI 316L SS) were selected for this study. Advanced characterization tools like SEM-EDAX, XPS, CLSM, DGGE and AFM imaging were used.

Experimental Scheme

The gross approach adopted for the present work can be divided into two parts as the following:

- Identify the preferential adhesion of Manganese manganese oxidizing bacteria (MOB) and natural microorganisms in seawater on polished and etched stainless steel surfaces and correlate with the microchemistry on the surface
- Differentiate the corrosion characteristics of stainless steels with and without MOB biofilms using electrochemical techniques and advanced microscopic techniques

In cooling water systems of nuclear power plants, and oil and gas industry austenitic 316L SS is popularly used as condenser material and pipelines. AISI 316L SS was considered as the main study material and its localized corrosion characteristics were compared with lesser corrosion resistant AISI 202 SS under biofilm forming conditions. The composition of these alloys is given in Table 1.

Table 1
Composition of Specimens used

Material	Composition wt %								
AISI 316L	Cr-17	Ni-12	Mn-1.5	C-0.03	Si-0.5	P-0.03	S-0.03	Mo-2.1	Fe-balance
AISI 304	Cr-18	Ni-8	Mn-1.8	C-0.03	Si-0.3	P-0.04	S-0.02	Mo- -	Fe-balance
AISI 202	Cr-14	Ni-1.0	Mn-8.8	C-0.1	Si-0.5	P-0.07	S-0.01	Mo-0.1	Fe-balance

The SS specimen surfaces were subjected to electrolytic etching according to ASTM E407 [21] to reveal the microstructure using an optical microscope (Leica, Germany). These etched surfaces were exposed to MOB cultures for biofilm formation. The main microbe selected for this study was a MOB isolated from surfaces of steel scraps in IGCAR storage yard and identified as Bacillus flexus IGCAR-01/2011 in the authors' laboratory.[19,22] The specimens withdrawn after 24 h were observed under optical microscope for combined visualization of enhanced adhesion and microstructure. Biofilms were stained with nucleic acid stain and examined using Epifluorescence epifluorescence microscope (Nikon E600) for understanding the morphology.[23] The growth curve of B. flexus IGCAR-01/2011 on the polished and etched SS specimens was estimated and fitted by the Gompertz modified equation as described elsewhere.[24,25] The fitting and the accuracy of the estimations was evaluated from determination coefficient (R^2). μ (decimal logarithm of the number of bacteria counts at time t) L (the specific growth rate in h), A (logarithmic population increase in cfu/day) and R^2 values and tabulated. The surface morphological characteristics and biofilms on the as polished and etched SS specimens were observed under scanning electron microscope (SEM) (NanoEye, Singapore) and EDX analysis was done for etched and polished SS surfaces with Esprit analysis program connected with SEM.

To understand the natural biofilm formation with special emphasis on adhesion of different manganese oxidizing bacteria in the seawater as polished and etched SS specimens were exposed to natural seawater in pump house of Nuclear Desalination Demonstration Plant (NDDP) located at Kalpakkam, India for two weeks and the density estimated using Mn agar procured from Himedia Laboratories, Mumbai. SS specimens (Polished polished and etched) with two week old natural seawater biofilm was were analyzed with CLSM (Zeiss 710 Confocal Spectral Microscope Imaging System, Carl Zeiss Microscopy GmbH, Jena, Germany) after staining as per procedure given by Jiang et al.[26] Four lasers (Argon, Diode 405-25, HeNe 543, HeNe 633) were used in this experiment. With the same excitation laser, the confocal data for protein (stained by FITC) and Carbohydrates (stained by Con A) were recorded simultaneously. The images of other biofilm components were recorded sequentially. 3-D and orthographic views of biofilms were reconstructed with Zen 2.0 analysis software. Biofilm Community analysis with Denaturing denaturing Gradient gradient Gel gel Electrophoresis electrophoresis (DGGE) was carried out for the seawater biofilms on different SS specimens as per procedure described elsewhere.[27]

Electrochemical techniques like cyclic potentiodynamic polarization (CPP) and potentiostatic polarization were carried out with MOB biofilms and as polished SS specimens in seawater electrolyte.as per ASTM standard G61-86[28] using a potentiostat Autolab type PGSTAT30, Ecochemie, The Netherlands. All the electrochemical experiments were done in the seawater (electrolyte) collected from the NDDP seawater pump house, Kalpakkam. Potentiostatic polarization experiments were carried out at 700 mV with respect to OCP of SS specimens with and without MOB biofilms. This experiment was carried out to study the pit morphology based on the influence of bacterial biofilm on the SS with different Mn concentrations. After visualizing the pit morphology on polarized specimens with optical microscope, the specimens were stained with acridine orange and using CLSM the 3D and 2D images of pits were captured. Electrochemical impedance spectroscopic (EIS) analysis was carried out for both the polished and SS specimens exposed to bacterial culture. Complex impedance data obtained from these measurements were analyzed by using FRA software and data were fit using Zman software.

X-ray Photoelectron photoelectron Spectroscopy spectroscopy (XPS) analysis (SPECS, Germany) was carried out on SS specimens (as polished, etched and exposed to *B. flexus* IGCAR-01/2011 grown in 10% minimal medium for four weeks) to confirm the Mn oxidation on

SS surfaces. SS specimens exposed to bacterial cultures were cleaned in a sonicator bath with absolute ethanol for removing all traces of biofilm and then XPS surface analysis of the specimens was carried out.[19]

Correlation of Biofilm characteristics and Surface Chemistry

The materials selected for this study was 202 SS and 316L SS. 316L SS are designed for service with high corrosion resistance in natural waters even with high chloride content.[29] The basic 300 series has 18% Cr and 8% Ni and 1-2 % Mn. Localized corrosion resistance of 316L SS is enhanced by adding 2-3% Mo and reducing carbon. However, many workers have observed failure of 316L SS pipes under the biofilms of MOBs and iron oxidizing bacteria (IOBs) in natural waters with 200 to 500 ppm chloride. [30,31] Hence it is essential to establish the role of biofilms of MOBs in pit initiation on 316LSS. Stainless steel grade 200 series containing 8 to 9% Mn are non-magnetic and have austenitic structure. 202 SS was selected for this study as an alloy with high Mn content.

Primary objective of this study was to identify the adhesion pattern of MOB *Bacillus flexus* on these two stainless steels with varying Mn concentration. Both as polished and etched surfaces were used for adhesion evaluation studies. Etching helped to accelerate dissolution of alloying component elements for studying enhancement of metal ions especially Mn ions on microbial adhesion. Etched surfaces also helped to identify preferential adhesion to different second phase particles. Optical micrographs of etched surfaces of 202 SS (Figure1a) revealed large number of MnS inclusions and second phase particles due to the higher percentage of Mn in these steels while 316L SS (Figure 1b) showed clean microstructure.

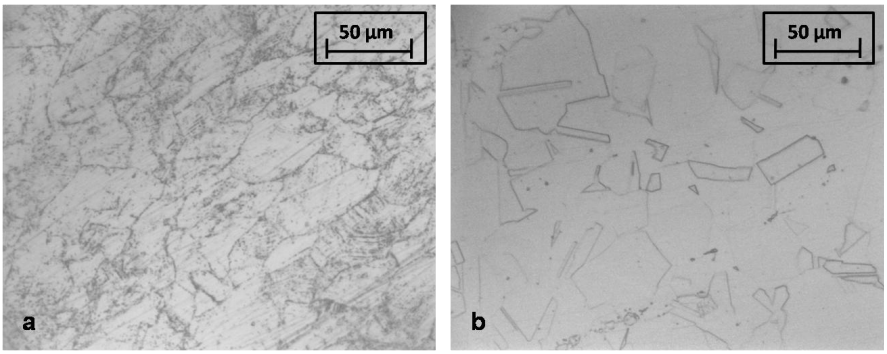

Figure 1: Optical Micrographs of Etched surfaces of a) 202SS b) 316L SS

Bacillus flexus is a gram-positive, rod shaped (Figure 2) sporulating microbial cell (size 2 µm) and its manganese oxidation property is confirmed by formation of blue color by leucoberbelin blue.

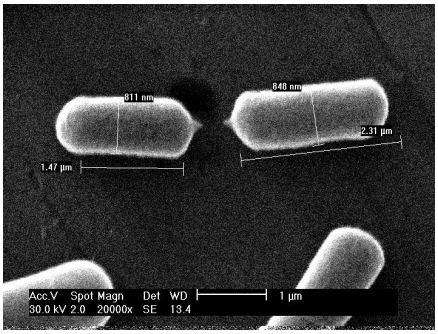

Figure 2: SEM of *Bacillus flexus* IGCAR-01/2011 on 304SS surfaces (scale – 1 µm)

The etched and polished specimens exposed for 24 h in the *B. flexus* culture was imaged with optical microscope to observe simultaneously the etching features and adhered bacterial cells. Table 2 shows that the etching enhanced bacterial adhesion and cell aggregation on the SS surfaces. The bacterial growth curve of *B. flexus* fitted by Gompertz modified equation on polished and etched SS surfaces is shown in Fig. 3. The density of MOB was the highest on etched 202SS with highest Mn content. Table 3 shows the Gompertz parameters (μ, *L, A)* and determination coefficient (R^2) of the adjusted modified Gompertz model to bacterial growth curves of cells on etched and polished SS surfaces. High R^2 (0.93 to 0.99) indicated the good fitting of experimental data to Gompertz model. Results obtained from fitting Gompertz equation to experimental data indicated that etching distinctly decreased Lag phase (*L*) and increased logarithmic population (*A*). Specific growth rate (μ) also increased for etched surfaces confirming enhanced and favorable growth of MOB *B. flexus* on these SS surfaces. This increase was proportional to the increased Mn content in the alloy and was the highest on 202 SS surface.

Table 2
Enumeration of cell aggregation and scattered cells on Polished and Etched 316L SS surfaces

Specimen Type	Average size of aggregation (m)	Average number of cells in aggregation
Polished 316L SS	12.5 卤 2.3	10 卤 2.2
Etched 316L SS	23.1 卤 4.4	72.1 卤 10.3

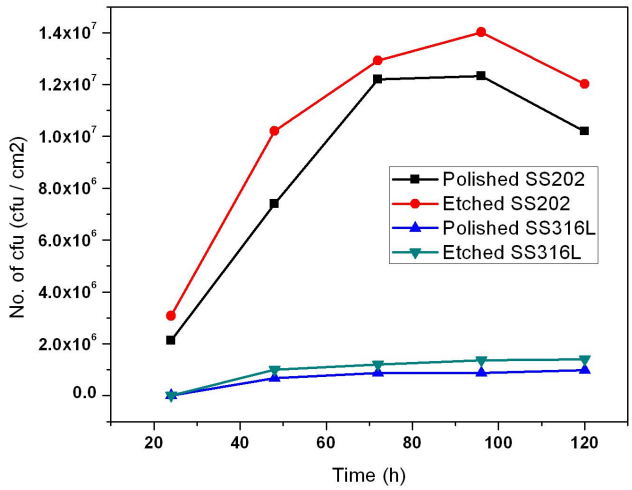

Figure 3: Growth pattern of B. flexus IGCAR-01/2011 on Polished and Etched 202SS & 316L SS surfaces

Epifluorescence micrograph of B. flexus biofilm on polished and etched 316L SS surface (Figure 4 a & b) further confirms visually the accelerated adhesion and actively growing cells on the etched surface. Number of orange fluorescing cells with high density of RNA depicts actively metabolizing cells[32].

Table 3
Gompertz Parameters (L, A) and determination coefficient (R^2) of the adjusted modified Gompertz model to bacterial growth patterns of B. flexus culture on Polished and Etched SS specimens

Specimens	(log CFU/cm^2/day)	*L* (h)	*A* (log CFU/cm^2)	R^2
Polished 202SS	1.16 ± 0.1 x 10^7	32.65 ± 4.11	0.063 ± 0.02	0.93
Etched 202SS	1.30 ± 0.7 x 10^7	28.86 ± 1.97	0.076 ± 0.01	0.97
Polished 316L SS	9.17 ± 0.3 x 10^6	40.08 ± 2.32	0.148 ± 0.01	0.98
Etched 316L SS	1.32 ± 0.6 x 10^7	39.72 ± 2.37	0.153 ± 0.03	0.99

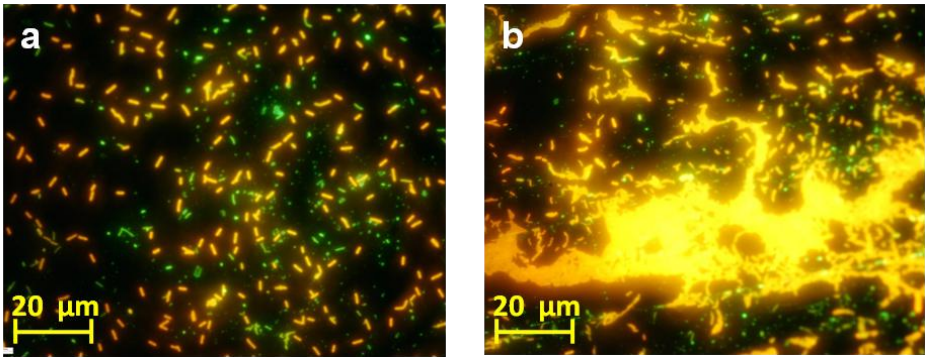

Figure 4: Epifluoromicrograph of 48 h biofilm of B. flexus IGCAR-01/2011 on a) Polished and b) Etched 316L SS surfaces

Scanning Electron Micrograph (Figure 5) showed preferential attachment of B. flexus **on the second phase particles** on etched AISI 202 surfaces in an early biofilm (24 h).

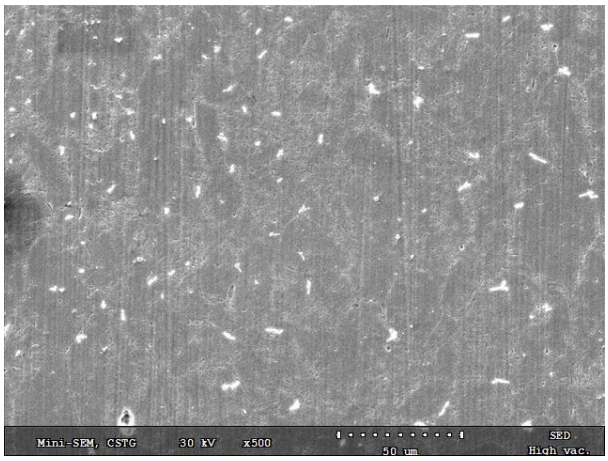

Figure 5: Scanning Electron Micrograph showing preferential attachment of *B. flexus* IGCAR-01/2011 along the grain boundaries and second phase particles on 24 h MOB biofilmed and etched 202 SS surfaces (scale - 50 m)

Table 4
Elemental analysis (EDAX) of as polished, etched and exposed to B. flexus IGCAR-01/2011

Type	Specimen	Chromium	Manganese	Iron	Nickel
Polished	202SS	13.14033	**11.1301**	68.57507	0.106591
	316SS	14.38997	2.237393	57.25936	7.215668
Etched	202SS	13.43158	**10.71066**	68.84779	0.375055
	316L SS	16.49202	2.057327	67.02502	9.3046
Etched & MOB Biofilmed	202SS	13.80769	**10.11623**	66.40241	0.632308
	316L SS	12.96192	2.045188	60.73109	9.1906

To explain the enhanced adhesion and growth rate of *B. flexus* on etched SS, surfaces chemistry of the surface was characterized by EDAX and XPS. EDAX analysis (Table 4) of the surface of etched SS showed a decrease in total Mn content and XPS analysis also showed decrease in metallic Mn. However XPS clearly showed an enhancement in the oxidized form of Mn which in turn favoured increased adhesion of MOBs. It is well established that chemical factors on the surface called as chemo attractants play an important role in microbial adhesion

Table 5
XPS of elemental analysis done on the surfaces of 202 SS and 316L SS specimens

Specimens									
202SS	**Cr-Mn-Fe Ratio**	**Cr atomic %**		**Mn atomic %**		**Fe atomic %**			
		O	**M**	**O**	**M**	**O**	**M**		
Polished	4.0 : 0.5 : 2.8	95	5	74	26	82	18		
Etched	3.3 : 0.9 : 8.6	88	12	88	12	78	22		
Etched and MOB biofilmed	5.0 : 0.0 : 1.3	92	8	0.0	0.0	63	37		
316L SS	**Cr-Fe-Ni-Mo Ratio**	**Cr atomic %**		**Fe atomic %**		**Ni atomic %**		**Mo atomic %**	
Polished	5.7: 6.5 : 1.0 : 0.6	89	11	69	31	24	76	69	31
Etched	3.7 : 8.2 : 0.5 : 0.4	84	16	78	22	0	100	63	37
Etched and MOB biofilmed	5.1 : 2.2 : 0.6 : 0.3	91	9	50	50	0	100	70	30

Detailed XPS characterization of passive film on polished, etched and etched and biofilmed 202 and 316 SS surface were carried out (Table 5). Biofilm was totally removed by ultrasonication before passive film characterization. On the polished 202 SS the surface oxide layer showed elemental peaks of Cr, Mn and Fe in the ratio of 4.0: 0.5: 2.8 where 74% of Mn is in +4 / +3 oxidation state with the remaining 26% as metallic. Oxygen peak showed the presence of 鈥 H bonding with the metallic elements apart from being as their respective oxides. On the etched 202 SS Cr, Mn and Fe was in the ratio 3.3: 0.9 : 8.6 where oxidized Mn has increased to 88% and oxidized form of Fe and Cr has decreased. On the etched and biofilmed surface the passive film showed the Cr, Mn and Fe ratio as 5.0:0:1.3 with total absence of Mn. Shi et al [15] has stated that MOB can selectively remove Mn by oxidation. XPS spectra in Figure 6 confirm the observation. Mn was below detection limit by XPS on 316L SS surface. However EDAX results showed similar trend.

Table 6
Total viability counts of heterotrophs and MOB on as polished and etched 202SS and 316L SS surfaces exposed to natural seawater

Specimen	**Seawater agar cfu/cm^2**	**Mn agar cfu/cm^2**
Polished 202SS	3.9 鈪 0.2 脳 10^3	1.5 鈪 0.4x 10^2
Etched 202SS	7.0 鈪 0.1 脳 10^3	2.3 鈪 0.2 脳 10^3
Polished 316L SS	3.6 鈪 0.3 脳 10^3	1.75 鈪 0.2 脳 10^2

Etched 316L SS	8.5 卤 0.5 脳 10^3	1.86 卤 0.1 脳 10^3

According to earlier studies, increase in surface roughness by electropolishing increased microbial adhesion. [34] To understand the effect of electrochemical etching on roughness AFM characterization of both polished and etched 202 SS was carried out. Results showed insignificant increase of 86 nm on etched surface from 52 nm on polished surface.

To understand the natural biofilm formation with special emphasis on adhesion of different manganese oxidizing bacteria in the seawater as polished and etched SS surfaces were also exposed to natural seawater. Estimation of total counts of heterotrophs and MOB (Table 6) further confirmed highest density on etched SS surfaces.

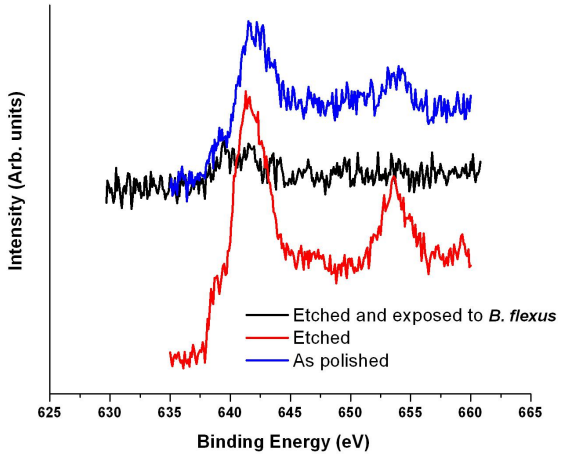

Figure 6: XPS spectra of 202SS specimens showing the presence of Mn on as polished and etched surfaces and no Mn on 202SS exposed to *B. flexus*

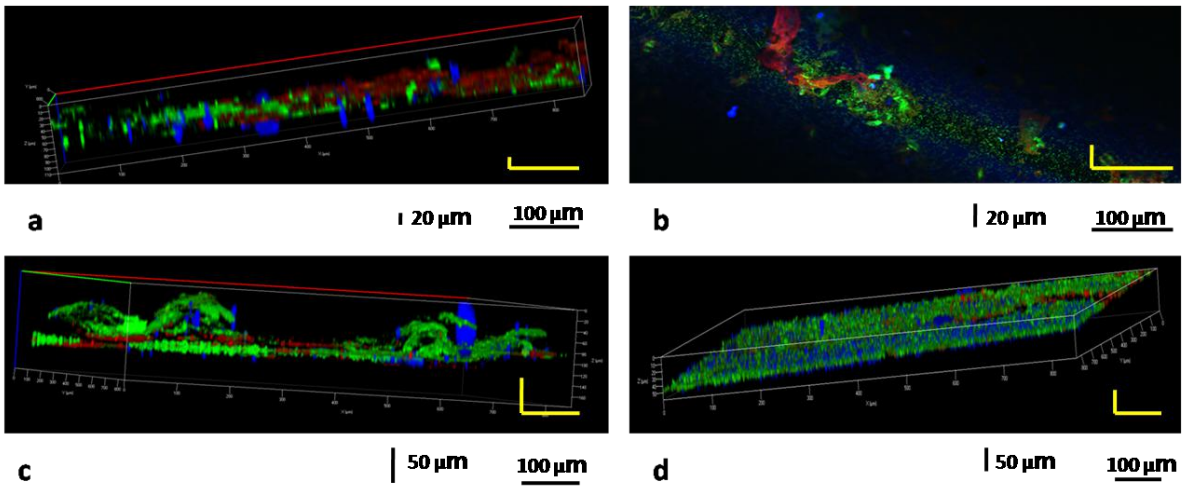

Figure 7: CLSM Micrograph showing biofilms on a) as polished 202SS, b) as polished 316L SS, c) etched 202SS, and d) etched 316L SS specimens exposed to natural seawater

CLSM imaging of seawater biofilmed 202SS and 316L SS (Figure 7) revealed interesting features. 202SS and 316L SS exposed to seawater for 2 weeks showed differences in thickness and coverage on the surfaces. The biofilm thickness on as polished 202SS and 316L SS surfaces were 110 and 50 µm respectively and on etched 202SS and 316L SS were 160 and 60 µm respectively. Thus the etched surfaces of both SS showed higher thickness and also showed complete coverage compared to patchy biofilms on as polished surfaces. Stains such as FITC and Calcofluor were used to examine the composition of biofilms where polysaccharides show red fluorescence and proteins show green fluorescence. CLSM images clearly showed predominance of proteins in biofilms formed on SS surfaces with higher protein content in the biofilms on the etched surfaces. Extracellular proteins are not only involved in developing biofilm architecture but also in the activation of enzymes and biofilm activity as reported. [35, 36] Thus biofilm activity along with thickness, density of microbes especially MOBs are higher on all etched surfaces of SS. Among the different SS surfaces 202 SS with highest amount of Mn had the highest values for all these biofilm parameters.

Electrophoretogram of V8 region of biofilm on polished and etched 202SS and 316L SS is shown in the Figure 8. V8 regions of etched 202SS (Figure 9c) and etched 316L SS (Figure 8d) showed higher intensity and probability of higher diversity of biofilm forming bacteria compared to polished specimens (Figures 8a & b).

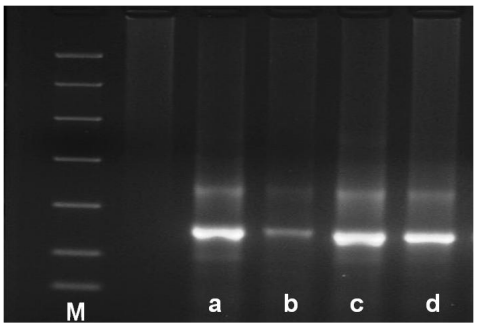

Figure 8: Electrophoretograph of amplified V8 regions of biofilms formed on a) as polished 202SS b) as polished 316L SS, c) etched 202SS, and d) etched 316L SS specimens exposed to natural seawater

Thus optical, epifluorescence and confocal microscopy and culturing and DNA isolation studies confirmed enhanced adhesion of MOB, thickness and coverage of MOB biofilm and microbial diversity on etched SS surfaces with highest values on etched 202 SS surface. EDAX analysis showed Mn reduction, and XPS analysis showed reduction in metallic Mn and increase in oxidized states of Mn on etched SS surfaces. This indicates that etching caused the oxidation of dissolved Mn from the surface. This higher amount of oxidized Mn favoured chemotactic adhesion of MOBs on the surface. Further the growth curve analysis of MOB on these surfaces indicated enhanced growth curve parameters like decrease in lag phase, increased logarithmic population and increased specific growth rate. Hence enhanced Mn ions on the surface helped in good proliferation of MOBs and biofilm formation. The MOBs further catalyzed Mn oxidation, however XPS spectra of passive film under the biofilm did not show Mn peak. Thus, accelerated Mn oxidation from the surface and inclusions under the influence of MOB biofilm can lead to pit initiation and propagation which was studied in detail in the second part of this paper. The iron content under the biofilm has also decreased due to pitting corrosion. Further, the SS surfaces were also exposed to seawater for confirming this enhanced adhesion of MOBs in natural environments. Exposure studies in seawater showed enhanced natural seawater biofilm

formation with higher density of MOBs on etched surfaces. Electrophoretogram confirmed higher diversity of MOBs on these surfaces. Thus detailed microbiological characterization confirms the preferential adhesion of MOBs and enhanced biofilm formation on SS surfaces which was found proportional to Mn content.

Corrosion & Pitting Characteristics

Second objective of the study was to identify the SS corrosion characteristics under these MOB biofilms with respect to location of pitting and pit density, depth and width using electrochemical and microscopic techniques.

Electrochemical techniques like electrochemical impedance analysis, CPP and potentiodynamic polarization were used to study as polished and biofilmed SS specimens. Accelerated electrochemical testing in seawater will give the probability and characteristics of long-term corrosion in natural environment. 48 h biofilm was selected as it represents the logarithmic growth phase of *Bacillus flexus*. Before CPP the specimens were subjected to EIS experiments. EIS spectra of MOB biofilmed 202SS and 316L SS specimens showed higher polarization resistance than as polished specimens inferring increased resistance due to biofilm formation. Cyclic potentiodynamic polarization (CPP) curves obtained for polished and etched 316L SS with 48 h *B. flexus* biofilm in sea water electrolyte is given in Figure 9a. Electrochemical parameters viz. OCP, passive current (I_{pass}), pitting potential (E_{pit}) and repassivation potential (E_{repass}) are given in the Table 7. CPP curve of polished 316L SS showed low passive current, noble OCP, and faster repassivation. CPP curve of biofilmed 316L SS showed increase in passive current, lowering of OCP and wider hysterisis indicating localized corrosion initiation and propagation. Figure 9b and Figure 11 c shows the pitting morphology under polarized biofilmed 316L SS. It appears that several smaller pits get initiated at numerous points to make a lacy pattern. According to Newman [1] this may be due to passivation and undercutting near pit mouths.

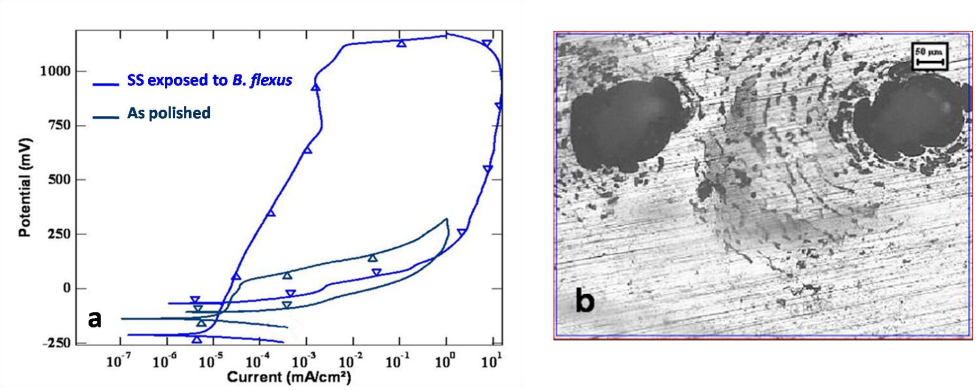

Figure 9: a) CPP curve of as polished 316L SS specimen and exposed to B. flexus IGCAR-01/2011 (seawater as the electrolyte) b) morphology of pits observed after CPP of MOB biofilmed 316L SS specimen (scale – 50 µm)

Table 7
Electrochemical parameters observed during cyclic potentiodynamic polarization of as polished and MOB biofilmed SS specimens

S. No.	Specimens	OCP	i_{pass} (μA cm^{-2})	E_{pit} (mV)	E_{repass} (mV)	Extent of Hysterisis (E_{pit} + E_{repass})
1.	As polished 202SS	- 180 mV	1 x 10^{-4}	- 65	- 275	340
2.	202SS + MOB Biofilm	- 255 mV	3 x 10^{-5}	+ 65	- 160	225
3.	As polished 304SS	- 140 mV	2 x 10^{-4}	+ 25	- 160	185
4.	304SS + MOB Biofilm	- 145 mV	6 x 10^{-5}	+510	- 70	580
5.	As polished 316L SS	- 145 mV	4 x 10^{-5}	+ 40	- 110	150
6.	316L SS+ MOB Biofilm	- 220 mV	6 x 10^{-3}	+1125	- 65	1190

As the biofilm forms on the surface the pitting potential is ennobled indicating a protective nature by the protein dominating biofilms in the initial stages. However once the MOBs have started manganese oxidation at the inclusions, pit initiation starts. Repassivation was difficult and area under the hysterisis curve is several times higher than the SS surface without biofilm. According to Frankel[37] difference between E_{pit} and E_{repass} shows the extent of hysterisis and the calculated values is shown in the Table 7. Etched and biofilmed 316L SS surface showed highest extent of hysterisis which is a measure of susceptibility to localized corrosion.

Potentiostatic polarization experiments were carried out at 700 mV with respect to OCP of SS specimens with and without bacterial biofilms. Figure 10 shows the SEM micrographs of potentiostatically polarized as polished and biofilmed 202 and 316L SS. Well defined deep pits were observed under biofilms and pits were observed close to bacterial aggregations. The current density curve with time showed highest current for biofilmed 202 SS (20.4 mA/cm^2) compared with polished 202 SS (16.3 mA/cm^2). Density of pits, width and depth of pits were also highest on biofilmed SS compared to polished SS surface.

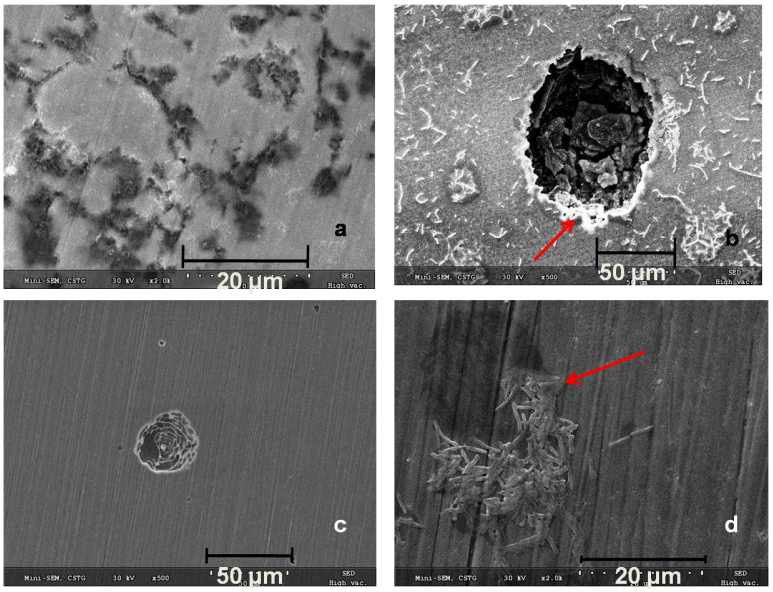

Figure 10: SEM micrograph of pits formed during potentiostatic polarization of a) as polished 202 SS, c) as polished 316L SS, b) MOB biofilmed 202 SS and d) 316L SS specimens. Arrows showing the pit initiation near bacterial cell aggregations

2D and 3D CLSM images of the pits on potentiodynamically polarized biofilmed 202SS and 316L SS is given in Figure 11. Pits on 202 SS had a depth of 300 µm and on 316L SS it was around 200 µm. Accelerated electrochemical studies with biofilmed SS surfaces and microscopic characterization have confirmed the enhanced localized corrosion susceptibility under biofilms of MOBs in seawater environments.

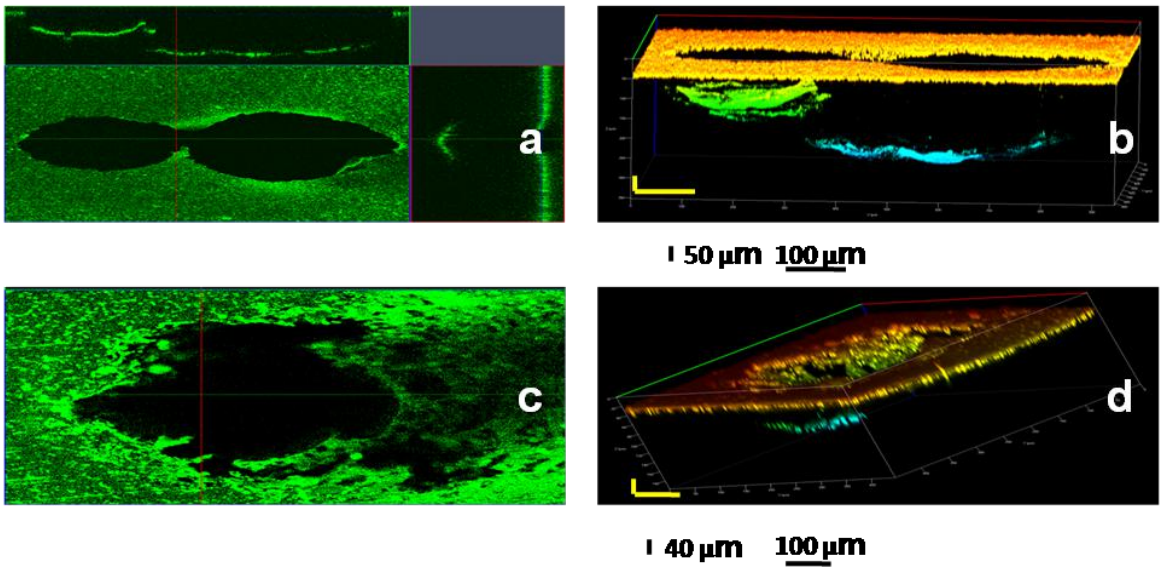

Figure 11: 2-D and 3-D CLSM micrograph of pits formed during CPP of a & b) MOB biofilmed 202SS; c & d) MOB biofilmed 316L SS specimens

Thus the Manganese oxidizing bacteria preferentially adhere to SS surfaces with higher amount of Mn in the surface and inclusions and oxidize the Mn and initiate pitting corrosion on SS surfaces. Thus the synergistic role of microstructure and MOBs in pitting corrosion of SS is confirmed in this study as represented in the scheme given below (Figure 12).

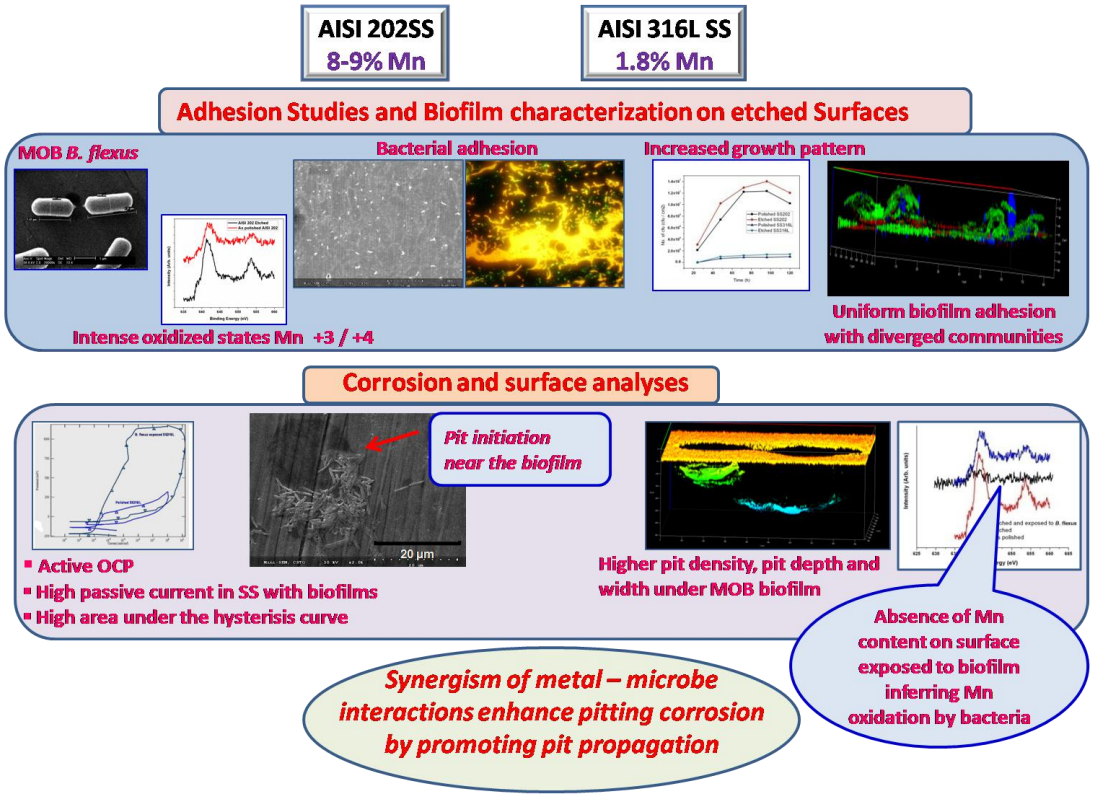

Figure 12. Schematic representation of Metal - Microbe Synergy on stainless steel surfaces

CONCLUSIONS

1. Advanced microscopic and molecular biology techniques confirmed enhanced adhesion, biofilm coverage, biofilm thickness, diversity and increased specific growth rate of manganese oxidizing *Bacillus flexus* on different SS surfaces and this was directly proportional to the Mn content on the surface of the SS.

2. Microscopic image of the biofilm on etched surface revealed preferential adhesion near second phases, inclusions and grain boundaries.

3. XPS and EDAX analysis confirmed decrease of Mn in the SS surface underbiofilms indicating Mn oxidation and utilization by MOBs that can result in pit initiations.

4. Electrochemical parameters like open circuit potential, passive current, repassivation potential and extent of hysterisis confirmed enhanced probability of pitting corrosion of SS under MOB biofilms.

5. Confocal laser scanning imaging and estimation of pit characteristics showed higher pit density, width and depth of pits under biofilms and pit formations closer to bacterial aggregations.

Thus an attempt on synergism of metal-microbe interaction enhancing pitting corrosion of stainless steels is confirmed.

ACKNOWLEDGEMENTS

Authors sincerely acknowledge Dr. S. Mahalingam and Dr. J. Sebastian Raja of India Institute of Technology-Madras, Chennai, India for providing CLSM facility. Authors also sincerely acknowledge Mr. Nanda Gopala Krishna for XPS analysis and Mr. A. Karthik for specimen preparation and Optical Microscopy analysis.

REFERENCES

1. R.C. Newman, “Understanding the corrosion of stainless steel”, NACE Corrosion, 57 12 (2001): p. 1030.

2. U. Kamachi Mudali, R. K. Dayal, J. B. Gnanamoorthy, S. M. Kanetkar, S. B. Ogale, “Localized Corrosion Studies on Laser Surface Melted Type 316 Austenitic Stainless Steel,” *Materials Transactions, JIM* 32, 9 (1991): P 845.

3. M.P. Ryan, N.J. Laycock, R.C. Newman, H.S. Isaacs, “The Pitting Behavior of Iron-Chromium Thin Film Alloys in Hydrochloric Acid”, *J. Electrochem. Soc*. 145 (1998): p. 1566.

4. J. Stewart, D.E. Williams, “The initiation of pitting corrosion on austenitic stainless steel: on the role and importance of sulphide inclusions”, *Corros. Sci*. 33, 3 (1992): p. 457.

5. N.J. Laycock, R.C. Newman, “Localised dissolution kinetics, salt films and pitting potentials”, *Corros. Sci*. 39 (1997): p. 1771.

6. B.J. Little, J.S. Lee, *Microbiologically Influenced Corrosion*, (John Wiley & Sons, Inc., Hoboken, NJ, USA 2007).

7. P. Linhardt, Pitting of stainless steels in fresh water influenced by manganese oxidizing microbes, DECHEMA Monographs (1996) p.

8. D. Walsh, E. Wills, T.V. Diepen, J. Sanders, “The effect of microstructure on microbial interaction with metals – accent welding”, CORROSION 94, paper no. 612.

9. M.P. Ryan, D.E. Williams, R.J. Chater, B.M. Hutton, D.S. McPhail, "Why stainless steel corrodes", *Nature* 415 (2002): p. 770.

10. M.A. Baker, J.E. Castle, “The initiation of pitting corrosion at MnS inclusions”, *Corros Sci*. 34 (1993): p. 667.

11. Pankaj Sharma, Himadri Roy, “Pitting Corrosion failure of AISI Stainless Steel Pointer Rod”, *Engineering Failure Analysis* 44 (2010): p. 400.

12. S.M. Gerchakov, B.J. Little, P. Wagner, “Probing Microbiologically Induced Corrosion” *Corrosion* 42 11 (1986): p. 689.

13. M.I. Suleiman, I. Ragault, R.C. Newman, “The pitting of stainless steel under a rust membrane at very low potentials”, *Corros. Sci*, 36 (1994): p.479.

14. W.H. Dickinson, F. Caccavo Jr., Z. Lewandowski, “The ennoblement of stainless steel by manganic oxide biofouling”, *Corros. Sci.*38 (1996): p.1407.

15. N. D. Tomashov, G.P. Chernova, *Passivity and Protection of Metals against Corrosion,* (Plenum Press, New York 1967), p.156.

16. Shi, X., Avci, R., Geiser, M. and Lewandowski, Z., Comparative study in chemistry of microbially and electrochemically induced pitting of 316L stainless steel, Corros. Sci., 45 (2003) pp. 2577-2595.

17. S.C. Dexter, K. Xu, G.L. Luther III, “Mn cycling in marine biofilms: effect on the rate of localized corrosion”, *Biofouling* 19 (2003): p. 139.

18. R.P George, P. Muraleedharan, S. Tamilvani, J. Brijitta, B.V.R. Tata, U. Kamachi Mudali, “Inhibition of manganese oxidizing bacterial adhesion on pretreated SS surfaces”, *Surface Engineering* 28*,* 3 (2012): p. 230.

19. B. Anandkumar, R.P. George, S. Tamilvani, N. Padhy, U. Kamachi Mudali, “Studies on microbiologically influenced corrosion of SS304 by a novel manganese oxidizer, *Bacillus flexus”*, *Biofouling* 27 (2011): p. 675.

20. S.J. Yuan, S.O. Pehkonen, “Microbiologically influenced corrosion of 304 stainless steel by aerobic *Pseudomonas* NCIMB 2021 bacteria: AFM and XPS study”, *Colloids Surf B: Biointerfaces* 59 (2007): p. 87.

21. ASTM E 407, “Standard Test Methods for Microetching Metals and Alloys” (West Conshohocken, PA: ASTM, 1989)

22. R.P. George, P. Muraleedharan, N. Parvathavarthini, H.S. Khatak, T.S. Rao, “Microbiologically influenced corrosion of AISI type 304 stainless steels under fresh water biofilms”, *Materials and Corrosion* 51, 4 (2000): p. 51.

23. A.D. Eaton, M.A.H. Franson, “Standard Methods for the Examination of Water & Wastewater”, (Washington, DC: American Public Health Association).

24. M.H. Zwietering, I. Jongenburger, F.M. Rombouts, K. Van’t Riet, “Modeling of bacterial growth curve”, *Appl. Environ. Biol*. 56, 6 (1990): p. 1875.

25. Tomac, R.H. Mascheroni, M.I. Yeannes, “Modeling the effect of gamma irradiation on the inactivation and growth kinetics of psychrotrophic bacteria in squid rings during refrigerated storage, Shelf-life predictions”, *J. Food Eng.*117 (2013): p. 211.

26. W. Jiang, S. Xia, L. Duan, S.W. Hermanowicz, "Biofilm architecture in a novel pressurized biofilm reactor", *Biofouling* 31, 4(2015): p. 321.

27. P. Balamurugan, M. Hiren Joshi, T.S. Rao, “Microbial fouling community analysis of the cooling water system of a nuclear test reactor with emphasis on sulphate reducing bacteria”, *Biofouling* 27, 9 (2011): p. 967.

28. ASTM G 61-86, “Standard Test Method for Conducting Cyclic Potentiodynamic Polarization Measurements for Localized Corrosion Susceptibility of Iron-, Nickel-, or Cobalt-Based Alloys” Designation: G 61 – 86 (West Conshohocken, PA: ASTM, 2009).

29. Z. Szklarska-Smialowska, *Pitting Corrosion of Metals*, (Houston,TX: NACE, 1986), p. 377.

30. G. Kobrin, “Corrosion by Microbiological Organisms in Natural waters”, *Mater. Perform.* 15, 7 (1976): p. 38.

C.M. Felder, A.A. Stein, 'Microbiologically Influenced Corrosion of Stainless Steel Weld an

1. C.M. Felder, A.A. Stein, 'Microbiologically Influenced Corrosion of Stainless Steel Weld and Base Metal--4 Year Field Test Results”, CORROSION/94, Paper no. 275, (Houston TX: NACE,1994).

2. C. Thien-Fah, G.A Mah, O’ Toole, “Mechanisms of biofilm resistance to antimicrobial agents”, *Trends Microbiol.* 9 (2001): p. 34.

3. M. Katsikogianni, Y.F. Missirlis, “Concise review of mechanisms of bacterial adhesion to biomaterials and of techniques used in estimating bacteria-material interactions”, *European Cells & Materials* 8 (2004): p. 37.

4. M. Momeni, M. Esfandiari, M.H. Moayed, “Improving pitting corrosion of 304 stainless steel by electropolishing technique”, *Iranian J. of Mater. Sci. & Engineering* 9, 4(2012) p. 34.

5. S.S. Branda, A. Vik, L. Friedman, R. Kolter, “Biofilms: the matrix revisited”, *Trends Microbiol*. 13 (2005): p. 20.

6. D.J. Lynch, T.L. Fountain, J.E. Mazurkiewicz, J.A. Banas, “Glucan-binding proteins are essential for shaping *Streptococcus mutans* biofilm architecture”, *Fems Microbiol Lett*. 268 (2007): p. 158.

7. G.S. Frankel, "Pitting Corrosion of Metals: A Review of the Critical Factors", *J. Electrochem. Soc*.145, 6 (1998): p. 2186.